ACS Photonics

pubs.acs.org/journal/apchd5

Article

Fast-Structured Illumination Microscopy Based on Dichotomy−Correlation Parameter Estimation (dCOR-SIM)

Jiaming Qian,[‖] Kailong Xu,[‖] Shijie Feng,* Yongtao Liu, Haigang Ma, Qian Chen,* and Chao Zuo*

Cite This: *ACS Photonics* 2024, 11, 1887−1892

Read Online

ACCESS | Metrics & More | Article Recommendations | Supporting Information

ABSTRACT: Structured illumination microscopy (SIM) has developed into one of the most significant super-resolution imaging techniques for studying the dynamics of live cells in the life sciences, thanks to the advantage of high photon efficiency. Usually, high-quality SIM super-resolution reconstruction presupposes accurate knowledge of the illumination parameters. However, the conventional iterative cross-correlation (COR) method requires cumbersome and time-consuming computations to realize reliable parameter estimation, posing a great challenge for fast, dynamic super-resolution imaging in complex scenes. In this letter, we propose an efficient and robust SIM algorithm based on dichotomy−correlation parameter estimation (dCOR-SIM), which significantly eliminates the iteration redundancy of conventional COR to enable low-complexity illumination parameter extraction while ensuring precision and noise immunity. Experiments demonstrate that dCOR-SIM can achieve high-accuracy parameter estimation with an efficiency ∼10 times better than conventional COR for fast, high-quality super-resolution reconstruction in complex experimental environments. We believe that dCOR-SIM, with its limited computational burden and robustness to noise, will facilitate fast, long-term live-cell super-resolution observations.

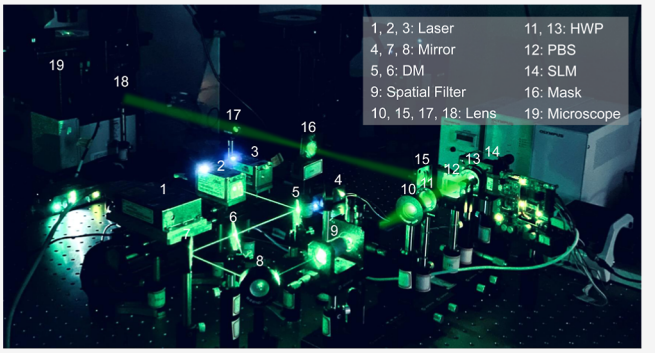

KEYWORDS: *structured illumination microscopy (SIM), parameter estimation, dichotomy, super-resolution*

Fluorescence microscopy plays an indispensable role in life sciences, but its lateral resolution is limited to ∼200 nm by the Abbe diffraction limit, which restricts the study of finer subcellular structures.[1] Over the past few decades, fluorescence super-resolution techniques have emerged to break the diffraction barrier and improve the spatial resolution of fluorescence microscopy to the nanometer level.[2−4] Among many fluorescence super-resolution techniques, structured illumination microscopy (SIM), with its unique advantages of full-field imaging and low photodamage, is well suited for long-term observation of organelle dynamics in live cells, thus attracting widespread attention in the field of biomedicine.[5−10]

Typically, SIM modulates the high-frequency spectra into the low-frequency region by using sinusoidal illuminations to achieve super-resolution. Solving or separating the different spectrum components of the sample and moving the high-frequency portion back to the correct position is a critical step in the SIM reconstruction algorithm.[11] This process is highly dependent on precise knowledge of the illumination parameters (wave vector, initial phase, and modulation depth), and even slight parameter errors can lead to severe artifacts in the reconstructed super-resolution image.[12−14] Many illumination parameter estimation algorithms, such as phase-of-peak (POP),[15] noniterative autocorrelation reconstruction (ACR),[16] and image recombination transform (IRT),[17] have been proposed to efficiently compute the illumination parameters. However, the compromised accuracy and sensitivity to low signal-to-noise ratios (SNRs) limit their practical application in SIM reconstruction algorithms. In contrast, the iterative cross-correlation (COR) algorithm, which searches for the wave vector coordinates with subpixel accuracy by iterative traversal and maintains a high level of accuracy and robustness even at low SNRs, has become one of the most widely used parameter estimation algorithms.[18,19] However, COR is computationally complex and time-consuming due to cumbersome iterative operations, which is not conducive to continuous dynamic observation of live cells, especially in complex experimental environments, where the illumination parameters cannot be calibrated at once. Recently, we proposed an iteration-free parameter estimation method based on principal component analysis (PCA) that allows fast and accurate parameter estimation at low SNRs.[20,21] However, the PCA method relies heavily on peak extraction of the ±1-order spectrum, the performance of which may degrade at

Received: December 14, 2023
Revised: March 13, 2024
Accepted: March 14, 2024
Published: April 1, 2024

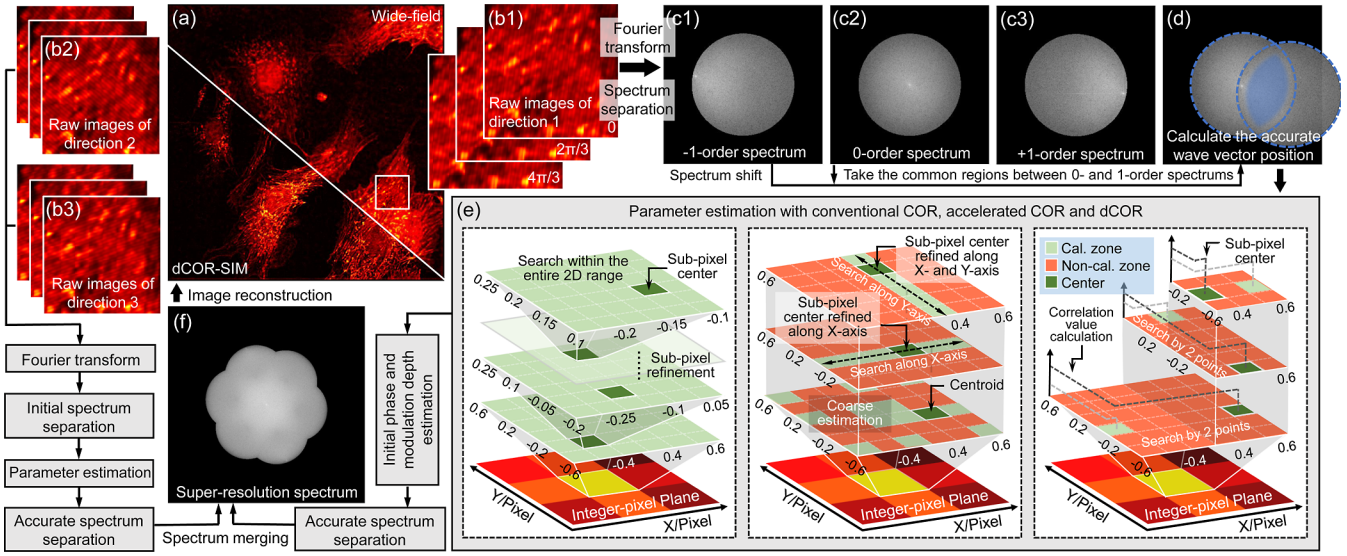

Figure 1. Flowchart of dCOR-SIM. (a) Wide-field image and the super-resolution image obtained by dCOR-SIM. (b) Raw SIM images in the first illumination direction from the white boxed region in (a). (c) Separated spectrum components. (d) Common areas of the 0- and 1-order spectrum components. (e) Flowchart of conventional COR, accelerated COR, and dCOR. (f) Merged super-resolution spectrum.

higher illumination frequencies or under total internal reflection fluorescent (TIRF) objective conditions. Therefore, it remains a major challenge to efficiently obtain accurate illumination parameters for fast, high-quality, super-resolution image reconstruction.

In this letter, we propose an efficient and robust SIM algorithm based on dichotomy−correlation parameter estimation (dCOR-SIM), which employs a dichotomous strategy to replace the intensive cross-correlation operations in the conventional COR-based parameter estimation method and significantly eliminates the iterative redundancy while ensuring accuracy and robustness. In conventional two-dimensional (2D) SIM reconstruction, the raw images are the fluorescence intensities of the sample excited by sinusoidal structured illuminations and modulated by the system point spread function (PSF) (Figure 1a,b). By introducing the three-step phase-shifting algorithm, the different spectrum components modulated by illuminations can be separated, where ±1-order spectra represent super-resolved information, as shown in Figure 1c (see Section S1 of the Supporting Information for details). However, these separated spectrum components cannot be directly used for super-resolution reconstruction due to the uncertainty of the illumination wave vector, initial phase, and modulation. For conventional COR, iterative cross-correlation operations in the form of real-space phase gradients are performed intensively to determine the wave vector with subpixel accuracy according to the fact that the common regions between the 0-order spectrum and the precisely frequency-shifted 1-order component have the maximum correlation value (Figure 1d). Since the common regions mainly distribute low-frequency information, which has a relatively high SNR because of the weak OTF attenuation, COR avoids the problems associated with spectrum degradation and, therefore, is robust to noise. However, COR usually requires hundreds of cross-correlation operations, which may take several times longer than regular image reconstruction, greatly affecting the efficiency of the entire SIM algorithm, especially in complex scenes (see Section S2 of the Supporting Information for details).

In order to improve the computational efficiency of parameter estimation, we proposed a coarse-to-fine accelerated COR algorithm, which roughly determined the wave vector by a few cross-correlation calculations and then gradually approximated the real coordinates by continuously narrowing the subpixel search interval (see Section S3 of the Supporting Information for details).[22] However, the coarse estimation of accelerated COR contributes only 3.4% of the resulting parameter estimation accuracy (taking the accuracy of conventional COR with 300 cross-correlation operations as a benchmark) with 25% (at least 13 cross-correlation computations) of the total computation, which also leads to more subsequent computations to localize the accurate wave vector. Note that the accuracy percentage represents the inverse of the ratio of errors. To further overcome the tradeoff between efficiency and accuracy, we propose a more efficient dichotomy-based parameter estimation scheme. Specifically, for the 1-order spectrum that has been compensated for the integer-pixel portion $\mathbf{k}_{\mathrm{int}}$ of the wave vector, we compute the correlation value between its version after being frequency-shifted by two specific subpixel shift vectors $\mathbf{k}_{\mathrm{p}}$ (which is also the initial value of the residual subpixel portion $\mathbf{k}_{\mathrm{sub}}$ of the wave vector) along the x direction and the 0-order spectrum, respectively, starting from the image center $(\mathbf{k}_{s,x}, \mathbf{k}_{s,y})$

$$\mathrm{Cor}(\mathbf{k}_p) = m\frac{\sum_{\mathbf{k}} \tilde{S}_0^*(\mathbf{k})\tilde{S}_{+1}(\mathbf{k} - \mathbf{k}_{\mathrm{sub}} + \mathbf{k}_p)\mathrm{e}^{\mathrm{i}\varphi_0}}{\sum_{\mathbf{k}} |\tilde{S}_0^*(\mathbf{k})\tilde{S}_0(\mathbf{k})|}, \tag{1}$$

$$\mathbf{k}_{p,x} \in \{\mathbf{k}_{s,x} - 0.5, \mathbf{k}_{s,x} + 0.5\}, \quad \mathbf{k}_{p,y} = \mathbf{k}_{s,y} \tag{2}$$

where Cor represents the cross-correlation operation, $\tilde{S}_0$ and $\tilde{S}_{+1}$ denote the 0- and +1-order spectrum components, respectively, $\mathbf{k}$ is the frequency coordinate, φ_0 is the initial phase, m is the illumination modulation, superscript * denotes the complex conjugate, and $\mathbf{k}_{p,x}$ and $\mathbf{k}_{p,y}$ are the components of $\mathbf{k}_p$ along the x and y directions, respectively. The larger correlation value is then utilized to search for an approximate solution $\mathbf{k}_{\mathrm{iter}}$ closer to $\mathbf{k}_{\mathrm{sub}}$

https://doi.org/10.1021/acsphotonics.3c01845
ACS Photonics 2024, 11, 1887−1892

$$\mathbf{k}_{\mathrm{iter},x} = \frac{\arg\max_{\mathbf{k}_{p,x}} \mathrm{Cor}(\mathbf{k}_{p,x}) + \mathbf{k}_{s,x}}{2} \tag{3}$$

where $\mathbf{k}_{\mathrm{iter},x}$ is the component of the updated shift in the x direction, and argmax represents the operation of searching for the maximum value. The updated value of $\mathbf{k}_{\mathrm{iter},y}$ in the y direction can be acquired by performing a similar operation, where the new starting point and shift vectors are as follows

$$(\mathbf{k}_{s,x}, \mathbf{k}_{s,y}) \leftarrow (\mathbf{k}_{\mathrm{iter},x}, \mathbf{k}_{s,y}) \tag{4}$$

$$\mathbf{k}_{p,x} \leftarrow \mathbf{k}_{\mathrm{iter},x}, \mathbf{k}_{p,y} \leftarrow \{\mathbf{k}_{s,y} - 0.5, \mathbf{k}_{s,y} + 0.5\} \tag{5}$$

In order to further refine $\mathbf{k}_{\mathrm{iter}}$, we perform the above dichotomy-based search with gradually decreased step spacing. In each update, the calculation interval will be halved, through which a more accurate wave vector can be accessed efficiently. It is worth mentioning that by adopting such a dichotomous operation, the accuracy of the wave vector is improved to ∼11% (about 3.2-fold enhancement) of the benchmark with the same computation volume as in the coarse estimation phase of accelerated COR, making it possible to achieve more accurate wave vector positioning with fewer cross-correlation calculations in the subsequent refinement phase. The details of the dichotomy-correlation-based (dCOR) parameter estimation algorithm are summarized as in Algorithm, where subscripts l and r are used to distinguish between two specific displacements along the x direction, and subscripts u and d are used for two specific displacements along the y direction. Figure 1e illustrates the comparative flowcharts of conventional COR, accelerated COR, and dCOR, from which we can intuitively see that, in contrast to conventional COR, which traverses the cross-correlation operations over a 2D region, accelerated COR only requires performing subpixel interpolation along two 1D line paths after a few 2D sparse computations, while dCOR further compresses the operations along the 1D paths to be performed at a few points along two lines, which reduces a large number of unnecessary computational redundancy and greatly improves the efficiency of parameter estimation. In addition, since the noise-robust cross-correlation operation is retained, dCOR maintains relatively excellent performance even at low SNRs. After obtaining the wave vector with subpixel accuracy by dCOR, the initial phase and modulation can then be calculated by complex linear regression (eqs S5 and S6 of the Supporting Information for details). Eventually, each spectrum component can be reorganized by the acquired illumination parameters, followed by a super-resolution image reconstruction (Figure 1f, eq S3 of the Supporting Information).

Algorithm 1 The dichotomy-correlation-based (dCOR) parameter estimation algorithm.

```
procedure INPUT(k_{s,x}, k_{s,y})
    k_{x_l} ← k_{s,x} − 0.5, k_{x_r} ← k_{s,x} + 0.5
    k_{y_d} ← k_{s,y} − 0.5, k_{y_u} ← k_{s,y} + 0.5
    k_{iter,x} ← (k_{x_l} + k_{x_r})/2, k_{iter,y} ← (k_{y_d} + k_{y_u})/2
    for Iter ← 1 to num do
        k_{p_l} ← (k_{x_l}, k_{iter,y}), k_{p_r} ← (k_{x_r}, k_{iter,y})
        if Cor(k_{p_l}) > Cor(k_{p_r}) then
            k_{x_r} ← k_{iter,x}
        else
            k_{x_l} ← k_{iter,x}
        end if
        k_{iter,x} ← (k_{x_l} + k_{x_r})/2

        k_{p_d} ← (k_{y_d}, k_{iter,x}), k_{p_u} ← (k_{y_u}, k_{iter,x})
        if Cor(k_{p_d}) > Cor(k_{p_u}) then
            k_{y_u} ← k_{iter,y}
        else
            k_{y_d} ← k_{iter,y}
        end if
        k_{iter,y} ← (k_{y_d} + k_{y_u})/2
    end for
    k_{s,x} ← k_{iter,x}, k_{s,y} ← k_{iter,y}
end procedure
```

We carried out a series of simulations to validate the performance of dCOR. The actually captured fluorescence image of bovine pulmonary artery endothelial (BPAE) cells was used to simulate the original SIM images acquired under a 40 × 0.6NA objective configuration, while Gaussian noises of increasing power were added to generate different SNR conditions. We first compared the performance of dCOR with that of accelerated COR in the coarse estimation stage. As shown in Figure 2a, the wave vector accuracy of dCOR is

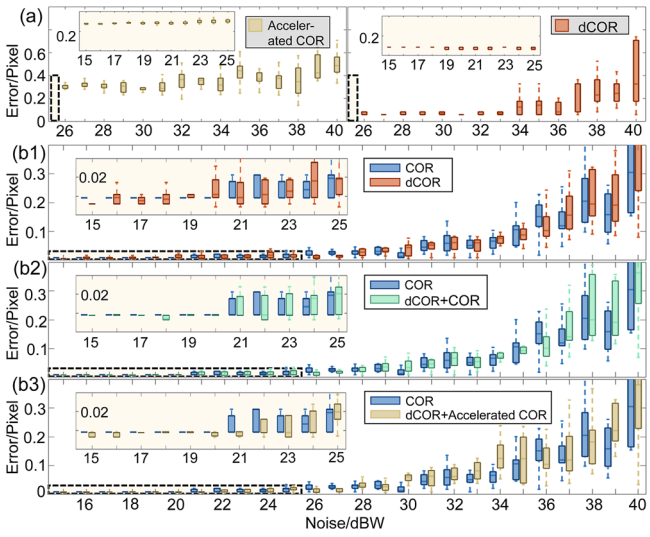

Figure 2. Wave vector errors estimated by different parameter estimation methods at different SNRs. (a) Wave vector errors of accelerated COR and dCOR in the coarse estimation phase. (b) Wave vector errors of convenient COR, dCOR, and combinations between COR, accelerated COR, and dCOR in the refinement phase. Simulations were repeated ten times independently with similar results.

∼0.08 pixels at regular SNRs, which is significantly better than that of accelerated COR (>0.27 pixels) with the same cross-correlation calculations. Then, we performed subpixel refinement using dCOR, accelerated COR, and conventional COR, respectively. The simulation results under different noise levels are shown in Figure 2b, where some crucial parameters, such as the cross-correlation computation counts, the final step spacing, and the accuracy at regular SNRs and at low SNRs, are listed in Table 1. It can be seen that dCOR achieves higher-precision wave vector estimation (approximately 0.006 pixels)

https://doi.org/10.1021/acsphotonics.3c01845
ACS Photonics 2024, 11, 1887−1892

Table 1. Performance Comparison of Different Parameter Estimation Methods

parameter estimation stage	method	cross-correlation calculation count	final step spacing (Pixel)	error at high SNRs (Pixel)	error at low SNRs (Pixel)
coarse phase	accelerated COR	13	0.5	0.2691 ± 0.0024	0.4268 ± 0.1820
	dCOR	13	0.125	0.0849 ± 0.0001	0.1540 ± 0.1747
fine phase	COR	300	0.025	0.0091 ± 0.0001	0.1130 ± 0.1237
	dCOR	29	0.015	0.0059 ± 0.0001	0.0976 ± 0.1171
	dCOR + COR	52	0.015	0.0089 ± 0.0001	0.0922 ± 0.0846
	dCOR + accelerated COR	32	0.015	0.0089 ± 0.0001	0.1258 ± 0.1103

with only 10% of the calculation amount of conventional COR, but maintains robustness to noise comparable to COR. It is worth mentioning that using dCOR for coarse estimation can significantly improve the performance and efficiency of conventional COR and accelerated COR (Figure 2b2,b3). The quantization results at different SNRs indicate that dCOR allows an accurate and robust estimation of the illumination parameters, thus realizing high-quality super-resolution image reconstruction, as shown in Figure 3. Note that when the

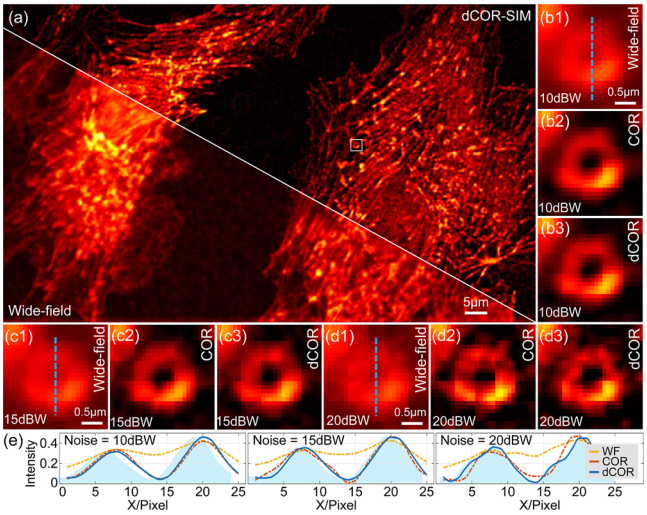

Figure 3. Simulation results of different parameter estimation methods. (a) Wide-field image and the super-resolution image obtained by dCOR-SIM. (b−d) Magnified wide-field images and super-resolution images from the white boxed region in (a) obtained by different methods at different SNRs. (e) Intensity profiles along the blue lines in (b−d), where "WF" represents "wide field". Simulations were repeated ten times independently with similar results.

difference in wave vector error is less than 0.01 pixel, the difference in reconstruction results is almost indistinguishable visually. In addition, we conducted another set of simulations using samples with simple, standard structures to more intuitively prove the advantages of dCOR over other parameter estimation methods, as shown in Figure S3 of the Supporting Information. These simulation results all demonstrate that dCOR has the best overall performance in terms of accuracy, efficiency, and noise immunity.

To further verify the validity of dCOR-SIM, we produced an interferometric SIM system (see Section S4 of the Supporting Information for details) and imaged a sample of fixed BPAE cells (with DAPI-labeled nucleus, Alexa Fluor 488-labeled actin, and MitoTracker Red CMX-Ros-labeled mitochondria). As shown in Figure 4a, the mitochondria and actin of BPAE cells appear blurred in the wide-field mode but can be well

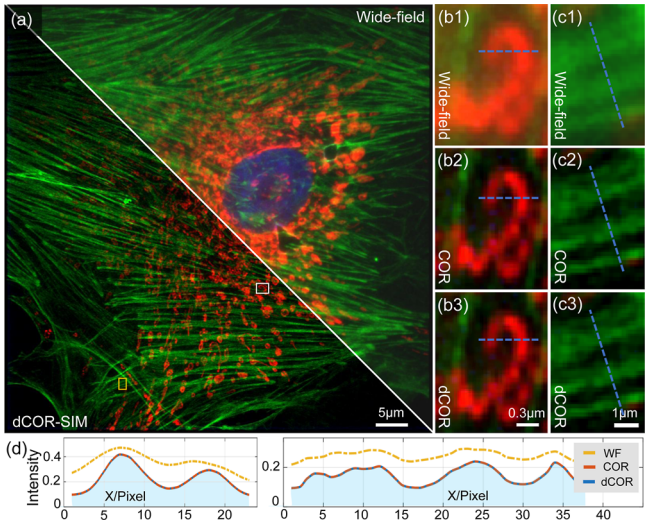

Figure 4. Comparison experiments on the super-resolution results of a fixed BPAE cell sample. (a) Wide-field image and the super-resolution image obtained by dCOR-SIM. The raw SIM images with a resolution of 1024 × 1024 were captured through a 100× objective (UPlanSApo 100×/1.40 Oil, Olympus, Japan). (b) Magnified wide-field image and super-resolution images from the white boxed region in (a) obtained by different methods. (c) Magnified wide-field image and super-resolution images from the yellow boxed region in (a) obtained by different methods. (d) Intensity profiles along the blue lines in (b,c), where "WF" represents "wide-field".

resolved in the super-resolution SIM mode. In addition, it can be seen from the comparison results between the conventional COR and the proposed dCOR that dCOR acquires almost comparable high-quality super-resolution images with an efficiency 10 times better than that of COR (Figure 4b,c). Finally, we applied dCOR-SIM to image the dynamics of live COS-7 (Origin Simian-7) mitochondria (labeled with MitoTracker Green FM). Figure 5 illustrates the reconstructed super-resolution images at different time points, which contain some interesting mitochondrial tubule fusion events. In Figure 5b, the mitochondrion indicated by the blue arrow established a connection with the right one by stretching its mitochondrial tubule, during which the connecting channel gradually thickened. Subsequently, this connection was temporarily disconnected but later reestablished, indicating variability in the mitochondrial dynamic network. Meanwhile, the two mitochondria marked by yellow arrows showed direct contact and fusion processes, reflecting the interaction and fusion behaviors between mitochondria. In Figure 5c, we can see that mitochondrial tubules explored and moved around when there were other mitochondrial tubules nearby. These phenomena are of significant importance for studying the basic functions of mitochondria.[23,24] See Video S1 for the complete mitochondrial dynamics. Section S5 of the Supporting Information

https://doi.org/10.1021/acsphotonics.3c01845
ACS Photonics 2024, 11, 1887−1892

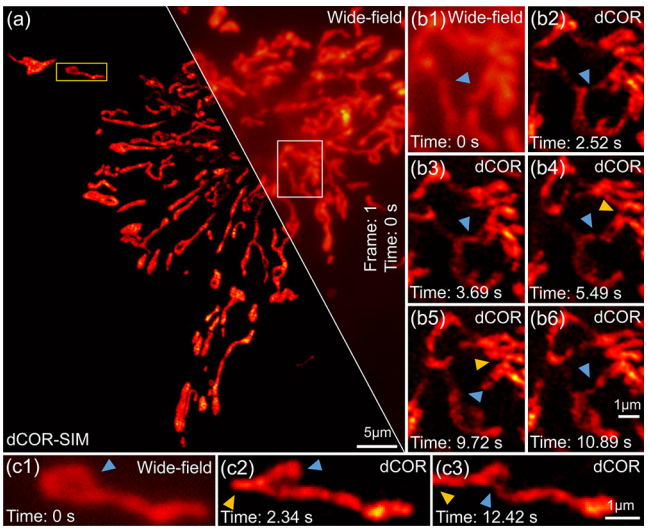

Figure 5. Super-resolution images of live COS-7 mitochondria at different time points (see also Video S1). (a) Wide-field image and the super-resolution image obtained by dCOR-SIM. The raw SIM images with a resolution of 512 × 512 were captured through a 60× objective (UPlanXApo 60×/1.42 Oil, Olympus, Japan). (b,c) Magnified super-resolution images from the white and yellow boxed regions in (a).

provides additional static and dynamic experiments. These experiments demonstrate that dCOR-SIM is capable of providing rapid illumination parameter corrections in live-cell dynamic experiments at about 10 times the efficiency of conventional COR, thus ensuring stable, high-quality super-resolution imaging in complex scenes.

In summary, we have proposed a dichotomy-correlation-based parameter estimation approach for fast SIM super-resolution reconstruction (dCOR-SIM). By optimizing the subpixel interpolation paths, dCOR-SIM can eliminate most of the unnecessary computational redundancy and provide more accurate illumination parameter estimation (less than 0.01-pixel wave vector error at regular SNRs) with only 1/10 of the conventional COR computation, while retaining robustness to noise. We believe that the efficient and robust performance makes dCOR-SIM important for realizing fast, long-term, and flexible super-resolution imaging of live cells.

■ ASSOCIATED CONTENT

Data Availability Statement

The data that support the findings of this study are available from the corresponding authors upon reasonable request.

Supporting Information

The Supporting Information is available free of charge at https://pubs.acs.org/doi/10.1021/acsphotonics.3c01845.

Principles of conventional structured illumination estimation algorithms and supplementary experiments (PDF)

Super-resolution images of live COS-7 mitochondria at different time points (MP4)

■ AUTHOR INFORMATION

Corresponding Authors

Shijie Feng − *Smart Computational Imaging (SCI) Laboratory, Nanjing University of Science and Technology, Nanjing, Jiangsu Province 210094, China; Smart Computational Imaging Research Institute (SCIRI) of Nanjing University of Science and Technology, Nanjing, Jiangsu Province 210019, China; Jiangsu Key Laboratory of Spectral Imaging & Intelligent Sense, Nanjing, Jiangsu Province 210094, China*; Email: ShijieFeng@njust.edu.cn

Qian Chen − *Jiangsu Key Laboratory of Spectral Imaging & Intelligent Sense, Nanjing, Jiangsu Province 210094, China*; Email: chenqian@njust.edu.cn

Chao Zuo − *Smart Computational Imaging (SCI) Laboratory, Nanjing University of Science and Technology, Nanjing, Jiangsu Province 210094, China; Smart Computational Imaging Research Institute (SCIRI) of Nanjing University of Science and Technology, Nanjing, Jiangsu Province 210019, China*; orcid.org/0000-0002-1461-0032; Email: zuochao@njust.edu.cn

Authors

Jiaming Qian − *Smart Computational Imaging (SCI) Laboratory, Nanjing University of Science and Technology, Nanjing, Jiangsu Province 210094, China; Smart Computational Imaging Research Institute (SCIRI) of Nanjing University of Science and Technology, Nanjing, Jiangsu Province 210019, China; Jiangsu Key Laboratory of Spectral Imaging & Intelligent Sense, Nanjing, Jiangsu Province 210094, China*; orcid.org/0000-0002-9110-4950

Kailong Xu − *Smart Computational Imaging (SCI) Laboratory, Nanjing University of Science and Technology, Nanjing, Jiangsu Province 210094, China; Smart Computational Imaging Research Institute (SCIRI) of Nanjing University of Science and Technology, Nanjing, Jiangsu Province 210019, China; Jiangsu Key Laboratory of Spectral Imaging & Intelligent Sense, Nanjing, Jiangsu Province 210094, China*; orcid.org/0000-0002-8229-5281

Yongtao Liu − *Smart Computational Imaging (SCI) Laboratory, Nanjing University of Science and Technology, Nanjing, Jiangsu Province 210094, China; Smart Computational Imaging Research Institute (SCIRI) of Nanjing University of Science and Technology, Nanjing, Jiangsu Province 210019, China; Jiangsu Key Laboratory of Spectral Imaging & Intelligent Sense, Nanjing, Jiangsu Province 210094, China*

Haigang Ma − *Smart Computational Imaging (SCI) Laboratory, Nanjing University of Science and Technology, Nanjing, Jiangsu Province 210094, China; Smart Computational Imaging Research Institute (SCIRI) of Nanjing University of Science and Technology, Nanjing, Jiangsu Province 210019, China; Jiangsu Key Laboratory of Spectral Imaging & Intelligent Sense, Nanjing, Jiangsu Province 210094, China*

Complete contact information is available at: https://pubs.acs.org/10.1021/acsphotonics.3c01845

Author Contributions

‖J.Q. and K.L. authors contributed equally to this work.

Funding

This work was supported by the National Natural Science Foundation of China (62227818, 62275125, 62275121, 12204239, and 62175109), the Youth Foundation of Jiangsu Province (BK20220- 946), Fundamental Research Funds for the Central Universities (30922010313), and the Open

Research Fund of Jiangsu Key Laboratory of Spectral Imaging & Intelligent Sense (JSGP202201).

Notes

The authors declare no competing financial interest.

■ ACKNOWLEDGMENTS

The authors would like to thank the editor and reviewers for their help on this paper.

■ REFERENCES

(1) Abbe, E. Beiträge zur Theorie des Mikroskops und der mikroskopischen Wahrnehmung. *Arch. Mikrosk. Anat.* **1873**, *9*, 413−468.
(2) Lichtman, J. W.; Conchello, J.-A. Fluorescence microscopy. *Nat. Methods* **2005**, *2*, 910−919.
(3) Zheng, G.; Horstmeyer, R.; Yang, C. Wide-field, high-resolution Fourier ptychographic microscopy. *Nat. Photonics* **2013**, *7*, 739−745.
(4) Shu, Y.; Sun, J.; Lyu, J.; Fan, Y.; Zhou, N.; Ye, R.; Zheng, G.; Chen, Q.; Zuo, C. Adaptive optical quantitative phase imaging based on annular illumination Fourier ptychographic microscopy. *PhotoniX* **2022**, *3*, 24.
(5) Heintzmann, R.; Cremer, C. G. Laterally modulated excitation microscopy: improvement of resolution by using a diffraction grating. *Optical Biopsies and Microscopic Techniques*, 1999; Vol. 3, pp 185−196.
(6) Gustafsson, M. G. Surpassing the lateral resolution limit by a factor of two using structured illumination microscopy: SHORT COMMUNICATION. *J. Microsc.* **2000**, *198*, 82−87.
(7) Li, D.; Shao, L.; Chen, B.-C.; Zhang, X.; Zhang, M.; Moses, B.; Milkie, D. E.; Beach, J. R.; Hammer, J. A.; Pasham, M.; et al. Extended-resolution structured illumination imaging of endocytic and cytoskeletal dynamics. *Science* **2015**, *349*, aab3500.
(8) Zhao, W.; Zhao, S.; Li, L.; Huang, X.; Xing, S.; Zhang, Y.; Qiu, G.; Han, Z.; Shang, Y.; Sun, D.-e.; et al. Sparse deconvolution improves the resolution of live-cell super-resolution fluorescence microscopy. *Nat. Biotechnol.* **2022**, *40*, 606−617.
(9) Wang, Z.; Zhao, T.; Hao, H.; Cai, Y.; Feng, K.; Yun, X.; Liang, Y.; Wang, S.; Sun, Y.; Bianco, P.; et al. High-speed image reconstruction for optically sectioned, super-resolution structured illumination microscopy. *Adv. Photonics* **2022**, *4*, 026003.
(10) Song, L.; Liu, X.; Xiong, Z.; Ahamed, M.; An, S.; Zheng, J.; Ma, Y.; Gao, P. Super-resolution reconstruction of structured illumination microscopy using deep-learning and sparse deconvolution. *Opt Laser. Eng.* **2024**, *174*, 107968.
(11) Chen, X.; Zhong, S.; Hou, Y.; Cao, R.; Wang, W.; Li, D.; Dai, Q.; Kim, D.; Xi, P. Superresolution structured illumination microscopy reconstruction algorithms: a review. *Light: Sci. Appl.* **2023**, *12*, 172.
(12) Huang, X.; Fan, J.; Li, L.; Liu, H.; Wu, R.; Wu, Y.; Wei, L.; Mao, H.; Lal, A.; Xi, P.; et al. Fast, long-term, super-resolution imaging with Hessian structured illumination microscopy. *Nat. Biotechnol.* **2018**, *36*, 451−459.
(13) Wen, G.; Li, S.; Liang, Y.; Wang, L.; Zhang, J.; Chen, X.; Jin, X.; Chen, C.; Tang, Y.; Li, H. Spectrum-optimized direct image reconstruction of super-resolution structured illumination microscopy. *PhotoniX* **2023**, *4*, 19.
(14) Cao, R.; Li, Y.; Chen, X.; Ge, X.; Li, M.; Guan, M.; Hou, Y.; Fu, Y.; Xu, X.; Leterrier, C.; et al. Open-3DSIM: an open-source three-dimensional structured illumination microscopy reconstruction platform. *Nat. Methods* **2023**, *20*, 1183−1186.
(15) Shroff, S. A.; Fienup, J. R.; Williams, D. R. Phase-shift estimation in sinusoidally illuminated images for lateral super-resolution. *J. Occup. Sci. Aust.* **2009**, *26*, 413−424.
(16) Wicker, K. Non-iterative determination of pattern phase in structured illumination microscopy using auto-correlations in Fourier space. *Opt. Express* **2013**, *21*, 24692−24701.
(17) Zhou, X.; Lei, M.; Dan, D.; Yao, B.; Yang, Y.; Qian, J.; Chen, G.; Bianco, P. R. Image recombination transform algorithm for superresolution structured illumination microscopy. *J. Biomed. Opt.* **2016**, *21*, 096009.
(18) Gustafsson, M. G.; Shao, L.; Carlton, P. M.; Wang, C. J. R.; Golubovskaya, I. N.; Cande, W. Z.; Agard, D. A.; Sedat, J. W. Three-Dimensional Resolution Doubling in Wide-Field Fluorescence Microscopy by Structured Illumination. *Biophys. J.* **2008**, *94*, 4957−4970.
(19) Wen, G.; Li, S.; Wang, L.; Chen, X.; Sun, Z.; Liang, Y.; Jin, X.; Xing, Y.; Jiu, Y.; Tang, Y.; et al. High-fidelity structured illumination microscopy by point-spread-function engineering. *Light: Sci. Appl.* **2021**, *10*, 70.
(20) Qian, J.; Cao, Y.; Bi, Y.; Wu, H.; Liu, Y.; Chen, Q.; Zuo, C. Structured illumination microscopy based on principal component analysis. *eLight* **2023**, *3*, 4.
(21) Lyu, J.; Qian, J.; Xu, K.; Huang, Y.; Zuo, C. Motion-resistant structured illumination microscopy based on principal component analysis. *Opt. Lett.* **2023**, *48*, 175−178.
(22) Qian, J.; Cao, Y.; Xu, K.; Bi, Y.; Xia, W.; Chen, Q.; Zuo, C. Robust frame-reduced structured illumination microscopy with accelerated correlation-enabled parameter estimation. *Appl. Phys. Lett.* **2022**, *121*, 153701.
(23) Wang, C.; Du, W.; Su, Q. P.; Zhu, M.; Feng, P.; Li, Y.; Zhou, Y.; Mi, N.; Zhu, Y.; Jiang, D.; et al. Dynamic tubulation of mitochondria drives mitochondrial network formation. *Cell Res.* **2015**, *25*, 1108−1120.
(24) Qin, J.; Guo, Y.; Xue, B.; Shi, P.; Chen, Y.; Su, Q. P.; Hao, H.; Zhao, S.; Wu, C.; Yu, L. ER-mitochondria contacts promote mtDNA nucleoids active transportation via mitochondrial dynamic tubulation. *Nat. Commun.* **2020**, *11*, 4471.

https://doi.org/10.1021/acsphotonics.3c01845
ACS Photonics 2024, 11, 1887−1892